An Improved Seastate Dependency For Surface Stress Derived from In Situ and Remotely Sensed Winds

Mark A. Bourassa

Center for Ocean-Atmospheric Prediction Studies, Florida State University, Tallahassee, FL 32306-2840, USA

ABSTRACT

An improved model is developed for the dependency of surface turbulent stress on wave characteristics. Recent studies have used differences between satellite and in situ observations to gain insights into the physical processes that might be related to air-sea interaction. Both scatterometers and buoys provide very accurate measurements of wind speed. Differences between these measurements can be explained in terms of the different mechanisms to which the instruments respond. A physically-based flux model is developed herein. Prior results suggest that the stress parameterizations, converting neutral equivalent wind speed to stress, applied to in situ observations differ subtlety from those that should be used for scatterometer-derived winds. These differences are due to water waves modifying the surface stress. This model provides a physical explanation of the observed differences, and provides a model for calculating stresses from scatterometer winds. The model is validated with recent in situ observations gathered under severe conditions. The model explains more wave-related variability in surface stress than previous models.

INTRODUCTION

Surface stress over water is primarily dependent on the vertical profile of wind speed, which is dependent on stratification of the atmosphere (atmospheric stability) and sea state (i.e., characteristics of the surface wave field). A typical assumption in GCM modeling of surface fluxes is that the wind and the waves are in a state of local equilibrium or a prescribed state of non-equilibrium. This assumption is equivalent to specifying a sea state. Recent examinations (Bourassa et al., 1999; Taylor and Yelland, 2001) based on in situ data have shown that this assumption is invalid for most spatial and temporal scales where there is substantial variability in sea state. Physical mechanisms have been proposed to account for the dependency of stress on sea state (Kusaba and Masuda, 1988; Geernaert et al., 1990; Toba et al., 1990; Perrie and Toulany, 1990; Maat et al., 1991; Smith et al., 1992; Yelland et al., 1998; Bourassa et al., 1999, 2001); however, an empirical formulation based on a much wider range of wind speeds and non-directional sea states (Taylor and Yelland, 2001) has been shown to provide substantially better matches to observations that cover a wide range of conditions. Differences between satellite and in situ wind observations have been used to infer the relative importance of several wave characteristics (Quilfen et al., 2001). The results of this study are correlations, which do not explain the physical mechanisms through which these wave characteristics modify surface fluxes. These differences also indicate that different parameterizations should be used to convert the observed wind speeds to stresses. A physical mechanism that utilizes these satellite-derived insights is developed, and it is found to be largely consistent with the results of Taylor and Yelland's (2001) empirical relation. One advantage of this physically-based mechanism is that it also considers directional sea state (i.e., the wind direction relative to the direction of wave propagation). This additional consideration makes the flux model consistent with observations over a wider range of conditions. The non-directional impacts on surface turbulent stress are developed and validated herein.

A stress-dependent model for significant wave height is coupled with a sea state dependent surface flux model to demonstrate the interdependence of surface fluxes and wave characteristics. It is shown that significant wave height

can be used, in conjunction with wind speed, as an indicator for the departure from local wind-wave equilibrium as well as the calculation of non-equilibrium fluxes. This result is largely consistent with the empirical formulation of Taylor and Yelland (2001); however, the physical impacts of sea state are parameterized through the influences of the surface's orbital motion induced by waves, rather than the slope of the waves. Such a model has been successfully applied to capillary-wave related surface stress (Bourassa et al., 1999); however, such wave dominate stress for ten meter wind speeds (U_{10}) < ~5 ms^{-1}. The mechanism was not applied to gravity wave related surface stresses, which dominate greater wind speeds due to the lack of appropriate data for validation. A recent study (Quilfen et al., 2001) has shown that the differences between observed and modeled scatterometer backscatter are well correlated to wave slope characteristics, but better correlated to the wave-induced surface motion. The modeled backscatter were found by inverting the geophysics model function (GMF) that was used to convert backscatter to vector winds. This model function has been shown be very accurate (Bourassa et al. 2003), indicating that small differences in wind speed (greater than ~5 cm/s), or the equivalent in backscatter, are likely to be due to physical differences rather than noise. These differences were binned according to low, moderate, and strong wind speeds. The correlations between these differences in backscatter, and the wave characteristics (orbital velocity and significant slope) were similar for low and moderate wind speeds; however, for strong winds the correlation was much better with orbital velocity (the significance of these differences was not given). This finding supports the physical reasoning applied in the flux model developed herein, for low wind speeds as well as high wind speeds.

DATA

The impacts of sea state on stress have previously been validated (Bourassa et al., 1999) for conditions dominated by capillary waves. The model reproduced observed changes in stress as a function of directional sea state. The developments in this study are applicable to conditions where stress is dominated by gravity waves. There are few observational data sets that contain both stress and wave observations. A preliminary version of observations from the Storm Wave Study experiment (SWS-2; Dobson et al., 1999; Taylor et al., 1999) was kindly provided by Peter K. Taylor. These observations have the additional advantage of covering a large range of wind conditions: 4 ms^{-1} to 24 ms^{-1}, with the quality control criteria described below. It is also the data set that Taylor and Yelland (personal communication, 2000) used to demonstrate that models using the HEXOS parameterization (e.g., Bourassa et al., 1999) overestimated stresses for high wind speeds.

The following constraints were applied to the SWS-2 observations.

1) The sonic anemometer's estimate of the speed of sound is between 332 and 338 ms^{-1},

2) The standard deviation of the platform's heading is less than 14°,

3) The dimensionless Monin–Obukhov scale length (z/L; eqs. 4-6) is less than 0.18.

They serve as quality control on the stress and wave observations, as well as remove conditions that were too far from neutral to be considered examinations of near-neutral conditions. The first constraint ensures that the speed of sound, which is critical to the calculation of turbulent fluxes, is within the range expected from the observed air temperatures (P. K. Taylor, pers. comm., 2003). The second constraint attempts to remove cases where excessive ship motion or flow distortion introduces too much variability in the observations; approximately 1% of the observations are removed due to this constraint (P. K. Taylor, pers. comm., 2003). The third constraint applies a measure of atmospheric stratification (z/L) to remove cases that are far from neutral stability, where the parameterizations that account for such departures are relatively uncertain.

FLUX MODEL

The downward momentum flux (τ) can be modeled in terms of the friction velocity ($\mathbf{u}_*$):

$$\tau = \rho \, \mathbf{u}_* \, | \, \mathbf{u}_* |, \tag{1}$$

where ρ is the density of the air. The upward surface turbulent fluxes of sensible (H) and latent heat (E) are

$$H = -\rho \, C_p \, \theta_* \, | \, \mathbf{u}_* |, \text{ and} \tag{2}$$

$$E = -\rho \, L_v \, q_* \, | \, \mathbf{u}_* |, \tag{3}$$

where θ_* and q_* are scaling parameters analogous to u_*, C_p is the specific heat of air, and L_v is the latent heat of vaporization. The goal of this study is to improve the accuracy of modeled values of u_*, which will improve the accuracy of these surface turbulent fluxes.

The direct influence of surface waves on flux and airflow characteristics ($\mathbf{u_*}$ and z_o) is determined by the relation between $\mathbf{u_*}$ and roughness length (z_o). Given $z_o(\mathbf{u_*})$ and the modified log wind relation $\mathbf{U}(z)$, where z is the height above the local mean surface, it is possible to iteratively solve for $\mathbf{u_*}(\mathbf{U})$ and $\mathbf{\tau}(\mathbf{U})$. The modified log–wind relation is

$$U(z) - U_s = \frac{u_*}{\kappa}\left[ln\left(\frac{z}{z_o} + 1\right) + \varphi(z, z_o, L)\right], \tag{4}$$

where k is von Kârmân's constant for momentum, and L is the Monin-Obukhov stability length. The influence of atmospheric stratification in the boundary-layer is modeled through the Monin-Obukhov stability length (Liu et al., 1979). The profiles of potential temperature (θ) and specific humidity (q) have functional forms similar to the log-wind profile.

$$\theta(z) - \theta_s = \frac{\theta_*}{k_\theta}\left[ln\left(\frac{z}{z_{o\theta}} + 1\right) + \varphi_\theta(z, z_{o\theta}, L)\right]; \text{ and} \tag{5}$$

$$q(z) - q_s = \frac{q_*}{k_q}\left[ln\left(\frac{z}{z_{oq}} + 1\right) + \varphi_q(z, z_{oq}, L)\right]. \tag{6}$$

The parameterizations of roughness lengths for potential temperature ($z_{o\theta}$) and specific humidity (z_{oq}), and L are identical to those used in the BVW (Bourassa-Vincent-Wood) flux model (Bourassa et al., 1999).

Dependence of stress on sea state

The dependence of stress on sea state (wave age, c_p / u_* in earlier versions of this model) typically enters through the gravity wave contribution in the roughness length parameterization (e.g., Kusaba and Masuda, 1988; Geernaert et al., 1990; Toba et al., 1990; Perrie and Toulany, 1990; Maat et al., 1991; Smith et al., 1992; Bourassa et al., 1999; Taylor and Yelland, 2001). The BVW roughness length (7) is among the most complicated: it is anisotropic and considers contributions to surface roughness from three types of surface features.

$$z_{o_i} = \beta'_v \frac{0.11\nu}{|u_{*_i}|} + \left[\left(\beta'_c \exp\left(\frac{-k\,f\,U_{orb}|\hat{e}_i|}{u_* \bullet \hat{e}_i}\right)\frac{b\,\sigma}{\rho_w|u_*||u_* \bullet \hat{e}_i|}\right)^2 + \left(\beta'_g \frac{0.48}{c_p/|u_{*_i}|}\frac{|u_*||u_* \bullet \hat{e}_i|}{g}\right)^2\right]^{0.5}. \tag{7}$$

where the β terms are binary weights for the roughness lengths associated with (from left to right) associated with an aerodynamically smooth surface (Nikuradse 1933; Kondo 1975), capillary waves (Bourassa et al. 1999), and gravity waves (Smith et al. 1992), where ν is the molecular viscosity of air, U_{orb} is the orbital speed of the dominant waves, b is a dimensionless constant (determined from laboratory observations; Bourassa et al. 1999), σ is surface tension, ρ_w is water density, c_p is the phase speed of the dominant waves, and g is gravitational acceleration. In this case, sea state (through orbital velocity) also influences the capillary wave roughness length. The orbital velocity term in the capillary wave roughness length simply changes the velocity frame of reference to that of a fraction f of the orbital velocity of the dominant waves. Laboratory studies (Okuda et al., 1997) have shown that must of the interactions between wind and waves occur near the crest of the dominant waves). This term in the model is analogous to modifying the lower boundary condition on velocity.

For $U_{10} > 7$ m s^{-1} the roughness length due to capillary waves is small compared to that for gravity waves. The BVW parameterization of capillary wave roughness length is dependent on the velocity frame of reference, which is often considered to match the surface current. However, the capillary waves and short gravity waves that interact with the airflow tend to ride on top of the dominant gravity waves. The exponential term in the capillary wave roughness length is an adjustment to the velocity frame of reference of the surface current. This frame of reference adjustment is the second mechanism through which sea state influences the roughness length.

Improvements to model

An improvement is made to the BVW (Bourassa et al. 1999) flux model. For high wind speeds, the BVW stresses were found to greatly overestimate the stresses observed in the Storm Wave Study experiment (SWS-2; Dobson et al., 1999; Taylor et al., 1999) experiment (P. K. Taylor, personal communication, 1999). Both Bourassa et al. (1999) and Taylor (personal communication, 1999) suggested that such biases were due to extrapolating the HEXOS parameterization for surface roughness length (Smith et al. 1992) to conditions for which it was not valid. The HEXOS parameterization is not applied in the model developed herein: the roughness length (8) can be written with no explicit dependence on sea state, where the gravity wave roughness length is a two-dimensional version of Charnock's

equation (Charnock, 1955). The influence of sea state enters solely through the modification of vertical shear in wind speed (9), due to a non-zero lower boundary condition: the wave-induced surface motion.

$$z_{o_i} = \left[\beta_v' \frac{0.11\nu}{|\mathbf{u}_{*_i}|} + \left[\left(\beta_c' \frac{b\,\sigma}{\rho_w |\mathbf{u}_*| |\mathbf{u}_* \bullet \hat{\mathbf{e}}_i|} \right)^2 + \left(\beta_g' \frac{a|\mathbf{u}_*| |\mathbf{u}_* \bullet \hat{\mathbf{e}}_i|^2}{g} \right)^2 \right]^{0.5} \right] \tag{8}$$

$$\left[\mathbf{U}(z) - f\,\mathbf{U}_{orb} - \mathbf{U}_{current} \right] \bullet \hat{\mathbf{e}}_i = \frac{\mathbf{u}_* \bullet \hat{\mathbf{e}}_i}{\kappa} \left[\ln\left(\frac{z}{z_{o_i}} + 1 \right) + \varphi(z, z_{o_i}, L) \right] \tag{9}$$

The orbital speed of gravity waves (U_{orb}) is approximated by

$$U_{orb} = \pi\,H_s\,/\,T_p, \tag{10}$$

where H_s is the significant wave height, and T_p is the period of the significant waves. For gravity waves, U_{orb} can easily be related to the significant slope used by Taylor and Yelland (2001). The fraction of the orbital velocity (f) that modifies the surface wind was set at 50% in BVW. There was considerable uncertainty in f, with little difference in the accuracy of fluxes for values of $f > 0.45$. Both f and a must be re-evaluated for use in (8).

The use of significant wave height in (10) is an oversimplification: H_s can be a combination of wind waves and swell from multiple sources. Directional differences in the wave spectra will contribute to errors in the estimated orbital velocity and consequently the errors in the stresses. However, wave spectra are rarely available from observational studies; whereas H_s is relatively common recorded in situ observations, and it is remotely sensed through altimetry. In practice, there are few sources of spectral wave information other than from wave models (e.g., WAMS; Gunther 1992; Janssen 1989, 1991) applied in operational weather centers.

The log-wind equation is in a more typical form, when the orbital velocity term is moved from the left hand side of (9) to the roughness length:

$$z_{o_i} = \left[\beta_v' \frac{0.11\nu}{|\mathbf{u}_{*_i}|} + \left[\left(\beta_c' \frac{b\,\sigma}{\rho_w |\mathbf{u}_*| |\mathbf{u}_* \cdot \hat{\mathbf{e}}_i|} \right)^2 + \left(\beta_g' \frac{a|\mathbf{u}_*| |\mathbf{u}_* \cdot \hat{\mathbf{e}}_i|^2}{g} \right)^2 \right]^{0.5} \right] \exp\left(-\frac{k\,\pi\,H_s\,f\,|\hat{\mathbf{U}}_{orb} \cdot \hat{\mathbf{e}}_i|}{T_p\,u_{*_i}} \right). \tag{11}$$

This version of the roughness length has an explicit dependency on sea state through the exponential dependence on the orbital velocity (or the ratio of H_s to T_p). However, there is a minor disadvantage associated with (11): changes of the sign of the stress, due to $U_{orb} > U(z)$, are not explicitly resolved. The sign of the stress components must then be determined by examining $U(z) - U_{orb}$.

COMPARISONS TO OBSERVATIONS

The model is evaluated with SWS-2 observations, and it is compared to empirical relation (12) developed by Taylor and Yelland (2001) based on the observations from SWS-2 and data from a wide range of other conditions. The functional form of the gravity wave portion of (11) is far different than the empirical relation (12):

$$z_o = 1200 H_S (H_S / \lambda_p)^{4.5}, \tag{12}$$

where λ_p is the wavelength associated with the dominant waves. Equation (12) has been shown (Taylor and Yelland, 2001) to be an excellent match to mean observations over a wide range of sea states. For moderate and high wind speeds, this empirical relation appears to be better than existing physically-based algorithms (Taylor and Yelland 2001); therefore, it is an excellent standard of comparison.

The roughness length can be estimated from the observed friction velocity and wind speeds. The impact of considering orbital velocity in (8) and (9), indicates that for the SWS-2 conditions the orbital velocity could have a large impact on the roughness length. The mean roughness lengths based on (11) are similar to the observed means and means based on (12). Both (11) and (12) are good representations of the mean roughness lengths.

A fit to the mean is not an ideal test for the quality of the roughness length parameterizations because the comparison roughness length is cross-correlated with the observed friction velocity. The substantial, but unknown, uncertainty in friction velocity leads to biases in the apparent dependence of observation-base roughness length on friction velocity. Accounting for this bias is beyond the scope of this study. This bias complicates the estimation of the constant in Charnock's parameterization (or the modified from in (11)), which is usually determined from the y-intercept of Fig. 1. For this preliminary study, the value of the modified a in (11) is approximated as 0.035, and $f = 0.8$.

These values are near to minima root mean square (rms) differences of observed friction velocity and drag coefficients. A slightly better fit to the mean SWS-2 observations could probably be achieved; however, it will be shown that this approximation is a considerable improvement over existing models.

The strong winds and atypically large drag coefficients (Fig. 1) seen in the SWS2 experiment are ideal for testing the influence of orbital velocity.
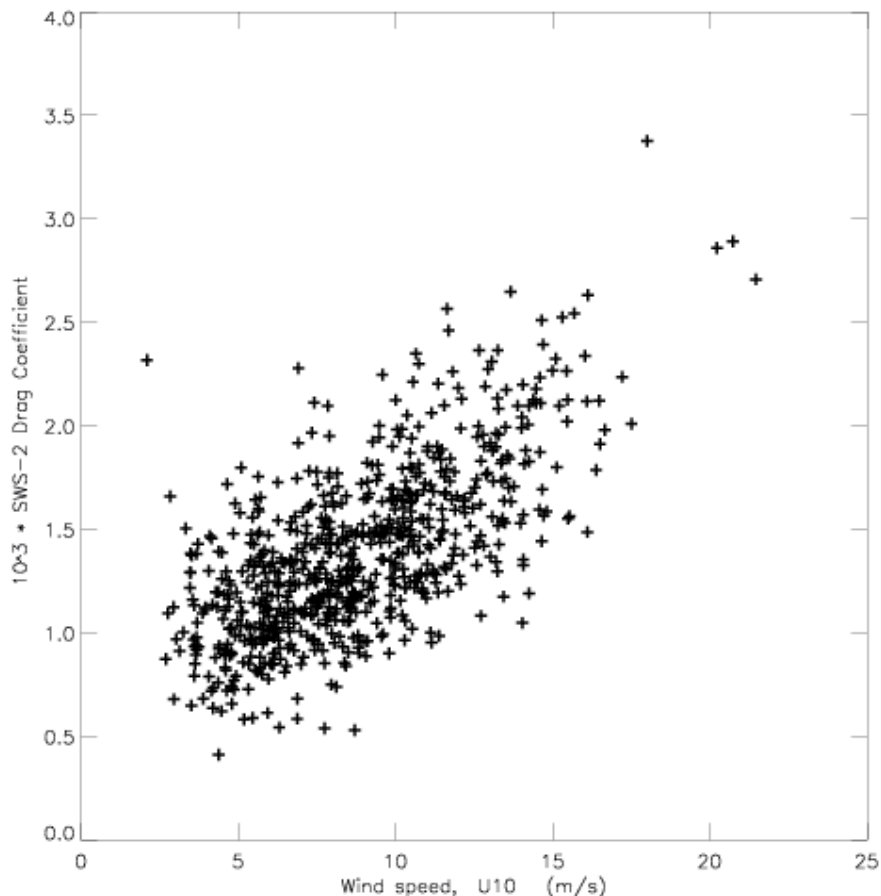

Fig. 1. SWS-2 drag coefficients as a function of wind speed. The variability in the drag coefficients and wind speeds is greater than typical for high quality in situ data sets.

Scatterplots of the modeled and observed friction velocities (Fig. 2) are useful for accessing the accuracy of the roughness length parameterizations through their influence of the modeled friction velocities. Comparison of the modeled and observed friction velocity is ideal because they avoid cross correlation. The friction velocities calculated with the Taylor and Yelland parameterization have a good fit to the mean (Fig. 3a); however, there is substantial variability (Fig. 2a) despite the wide range of wind and wave conditions for which the model is applicable. The model developed herein has a modestly better fit to the mean (Fig. 3b), with substantially smaller variability from the observed values. For $0.6 < u_* < 0.8$, there is a substantial bias between the two parameterizations, with the Taylor and Yelland parameterization overestimating the observed values. Taylor and Yelland's parameterization provides a better match to the extreme friction velocities ($u_* \approx 1.0$); however, there are very few observations (4), and the overestimation for $0.6 < u_* < 0.8$ is inconsistent with the good fit for larger friction velocities.
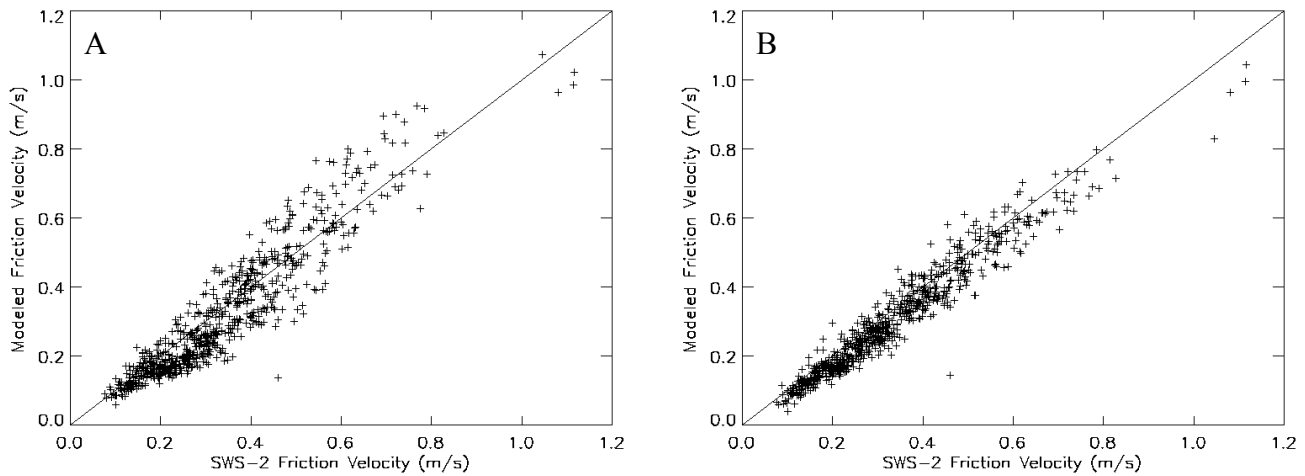
Fig. 2. Comparisons of observed and modeled friction velocity, based on SWS2 observations. Friction velocity derived with the (A) Taylor and Yelland 2001, (B) the model derived herein.
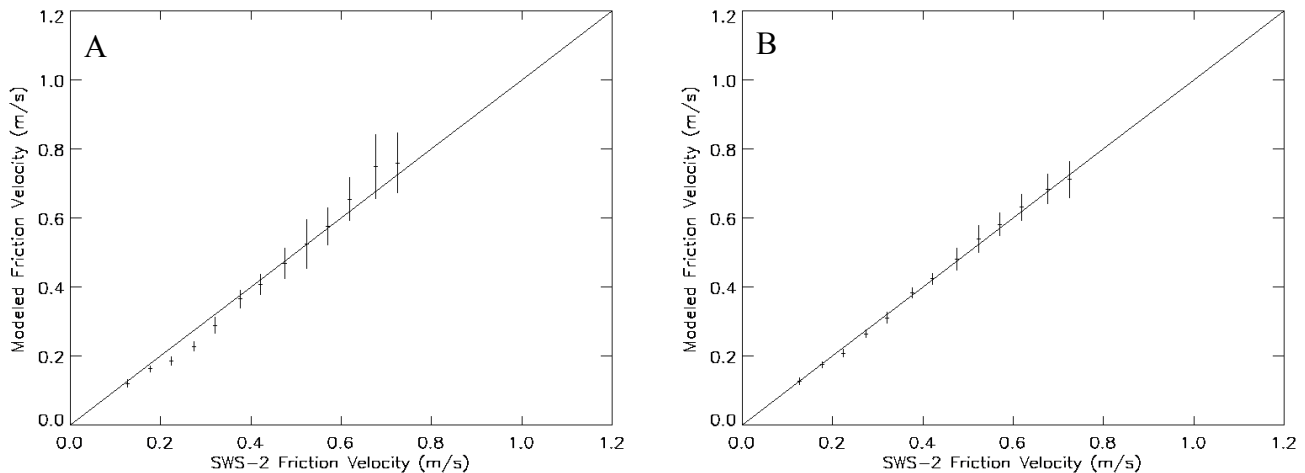

Fig. 3. Comparisons of means, within 0.05 bins of friction velocity, for SWS-2 observed friction velocity versus (A) Taylor and Yelland 2001, (B) the model derived herein. Bins must have ≥8 observations to be shown. The error bars indicate ±3 standard deviations in the mean.

Values for the standard deviations (Fig. 3) indicate that the model developed herein has substantially smaller variability from the binned means (Table 1).

CONCLUSIONS

Insights gained from examining the differences between satellite and in situ observations demonstrated a consistency with theory that had previously only been tested for low and moderate wind speeds. These observations and theory indicated that the orbital velocity of waves modifies wind shear, and consequently modifies oceanic surface turbulent stress. This concept had been difficult to verify because there were few appropriate in situ observations. The SWS-2 observations provide an excellent opportunity to test a model that considers orbital velocity. A physically-based model that considers orbital velocity is developed. Comparisons to the SWS-2 data find that the model developed herein has mean distributions similar to Taylor and Yelland's impressive empirical formulation. However, the new model's rms difference to roughness length is ~35% smaller than rms differences achieved by Taylor and Yelland: the new model better accounts for variability from the mean. Similarly, the uncertainty in the new model's friction velocity is much smaller than that of Taylor and Yelland's parameterization. Further work is required to optimize parameters in the new model; however, even with the estimates used herein, the new model is a substantial improvement over existing models.

Table 1. Uncertainty in the mean friction velocity, within 5 cm s^{-1} bins, specified by SWS2 friction velocity. The SWS2 standard deviation is limited by the bin width, causing the values to be much smaller than for the modeled friction velocities.

SWS2 bin mean (ms^{-1})	Number in bin	Standard Deviations in Mean (cm s^{-1})		
		BVW03	TY	SWS2
0.1267	63	0.32	0.34	0.18
0.1772	95	0.28	0.28	0.16
0.2234	89	0.36	0.44	0.14
0.2737	104	0.36	0.48	0.15
0.3213	83	0.54	0.77	0.16
0.3755	70	0.50	0.83	0.17
0.4215	63	0.56	0.98	0.19
0.4744	51	1.1	1.5	0.21
0.5234	26	1.3	2.4	0.30
0.5698	28	1.1	1.8	0.23
0.6195	22	1.3	2.1	0.30
0.6756	10	1.4	3.1	0.55
0.7247	10	1.7	2.9	0.43

The above results explain the differences in satellite and in situ wind observations. The stress associated with these wind observations must be identical, indicating that different parameterization, for converting wind speed to stress, should be used for these two types of observations. The model developed herein provides the physical basis for understanding these differences: the orbital velocity of water waves modifies the frame of reference (the bottom boundary condition) for wind speed. For in situ observations, a fraction (~80%) of the orbital velocity should be subtracted from the wind vector. However, for scatterometer observations, this modification of the scatterometer vector wind appears to be unnecessary, making the calculation of surface stress remarkably easier than for in situ wind observation

REFERENCES

Bourassa, M. A., D. G. Vincent, and W. L. Wood, A flux parameterization including the effects of capillary waves and sea state. *J. Atmos. Sci*., **56**, 1123-1139, 1999.

Bourassa, M. A., D. G. Vincent, and W. L. Wood, A sea state parameterization with capillary waves and non-arbitrary wave age. *J. Phys. Oceanogr*., **31**, 2840-2851, 2001.

Bourassa, M. A., D. M. Legler, J. J. O'Brien, and S. R. Smith, 2003: SeaWinds Validation with Research Vessels, *J. Geophys. Res.*, in press.

Charnock, H., Wind stress on a water surface. *Quart. J. Roy. Meteor. Soc.*, **81**, 639−640, 1955.

Dobson, F. W., R. J. Anderson, P. K. Taylor, and M. J. Yelland, Storm Wind Study II: Open ocean wind and sea state measurements. *Proc. Symp. on the Wind-Driven Air-Sea Interface: Electromagnetic and Acoustic Sensing, Wave Dynamics and Turbulent Fluxes,* M. L. Banner, Ed., University of New South Wales, 295-296, 1999.

Geernaert, G. L., Measurements of the angle between the wind stress vector in the surface layer over the North Sea. *J. Geophys. Res*., **91**, 7667−7679, 1990.

Günther, H., P. Lionello, P. A. E. M. Janssen, L., Bertotti, C. Brüning, J. C. Carretero, L. Cavaleri, A. Guillaume, B. Hansen, S. Hasselman, K. Hasselman, M. de las Heras, A. Hollingsworth, M. Holt, J. M. Lefevre, and R. Portz, 1992: Technical Report No. 68: Implementation of a third generation ocean wave model at the European Centre for Medium−Range Weather Forecasts, European Centre for Medium−Range Weather Forecasts, pp. 34.

Janssen, P. A. E. M., 1989: Wave-induced stress and the drag of airflow over sea waves. *J. Phys. Oceanogr.*, **19**, 745−754.

⎯⎯⎯⎯⎯⎯⎯⎯⎯, 1991: Quasi−linear theory of wind−wave generation applied to wave forecasting. *J. Phys. Oceanogr.*, **21**, 1631−1642.

Kusaba, T., and A. Masuda, The roughness height and drag law over the water surface based on the hypothesis of local equilibrium. *J. Phys. Ocean. Soc. Japan*, **44**, 200−214, 1988.

Kondo, J., Air−sea bulk transfer coefficients in diabatic conditions. *Bound.−Layer Meteorol.*, **9**, 91−112, 1975.

Liu, W. T., K. B. Katsaros, J. A. Businger, Bulk parameterization of air-sea exchanges of heat and water vapor including the molecular constraints at the interface. *J. Atmos. Sci*., **36**, 1722−1735, 1979.

Maat, M., C. Kraan, and W. A. Oost, The roughness of wind waves. *Bound.−Layer Meteorol*., **54**, 89−103, 1991.

Nikuradse, J., *Stromungsgesetze in rauben Rohren*. V. D. I. Forschungsheft 361, 22 pp., 1933.

Okuda, K., S. Kawai, and Y. Toba, 1997: Measurements of skin friction distribution along the surface of wind waves. *J. Oceanog. Soc. Japan*, **33**, 190-198.

Perrie W., and B. Toulany, Fetch relations for wind−generated waves as a function of wind−stress scaling. *J. Phys. Oceanogr.*, **20**, 1666−1681, 1990.

Quilfen Y., B. Chapron, and D. Vandemark, The ERS scatterometers wind measurement accuracy: evidence of seasonal and regional biases. *J. Atmos. Oceanic Technol*., **18**, 1684−1697, 2001.

Smith, S. D., R. J. Anderson, W. A. Oost, C. Kraan, N. Maat, J. DeCosmo, K. B. Katsaros, K. L. Davidson, K. Bumke, L. Hasse, and H. M. Cadwick, Sea surface wind stress and drag coefficients: the HEXOS results. *Bound.−Layer Meteorol*., **60**, 109−142, 1992.

Toba, Y., N., N. Ida, H. Kawamura, N. Ebuchi, and I. S. F. Jones, Wave dependence of sea-surface wind stress. *J. Phys. Oceanogr*., **20**, 705−721, 1990.

Yelland, M. J., B. I. Moat, P. K. Taylor, R. W. Pascal, J. Hutchings, and V. C. Cornell, Wind stress measurements from the open ocean corrected for airflow distortion by the ship. *J. Phys. Oceanogr*., **28**, 1511−1526, 1998.

Taylor, P. K., and M. J. Yelland, F. W. Dobson, R. J. Anderson, Storm Wind Study II: Wind stress estimates from buoy and ship. *Proc. Symp. on the Wind-Driven Air-Sea Interface: Electromagnetic and Acoustic Sensing, Wave Dynamics and Turbulent Fluxes,* M. L. Banner, Ed., University of New South Wales, 353-354, 1999.

Taylor. P. K., and M. J. Yelland, The dependence of sea surface roughness on the height and steepness of the waves, *J. Phys. Oceanogr*., **18**, 572−590, 2001.